Effects of Fault Current Limiters in Transient Stability Performance of Hybrid Wind Farm

Chintan R. Mehta, Bhavik D. Nathani, Prasad D. Deshpande, Santosh C. Vora

Abstract*: Low voltage ride through capability is an ability of the wind farm to stay connected with grid at the time of disturbance in the power system. The penetration of wind based renewable energy resources is increasing and the low voltage ride through consideration is vital for systems studies. The literature available demonstrates the improvement in low voltage ride through either by using fault current limiters or by implementing a control strategy for induction generator based wind farms. In this paper the low voltage ride through capability enhancement of the fixed speed induction generator is presented with various fault current limiters. The authors have presented the effects of fault current limiters in the aggregated hybrid wind farm consisting the combination of fixed speed induction generators and doubly fed induction generators which is not available in literature so far. A transient fault is simulated using PSCAD/EMTDC software in both the cases and the results are presented and discussed.

Keyword*: Doubly Fed Induction Generator (DFIG), Fault Current Limiters (FCLs), Fixed Speed Induction Generators (FSIG), Low Voltage Ride Through (LVRT)

I. INTRODUCTION

The penetration of renewable energy sources in power generation have increased due to technological developments and affordability in recent times due to environmental concerns. The bulk renewable power generation is mainly achieved through solar and wind farms. As the penetration of renewable energy generation is increased the transmission system operators (TSOs) have specified grid code requirements for integration of wind energy based power plants (WPP) in the grid. Low voltage ride through (LVRT) is one of the grid code requirements for the integration of WPPs. According to this requirement, WPPs should stay connected to the grid and inject reactive power to support the voltage at point of common coupling (PCC) during the fault [1][2]. Induction generator based technologies are used in wind energy based power generation, which includes fixed speed induction generators (FSIG) and doubly fed induction generators (DFIG). In past few decades, doubly fed induction generator has dominated the world's market in wind energy generation [3]. However, there are many WPPs installed with FSIG based WPPs. Although the FSIGs exhibit simple and robust construction features, it suffers from poor performance with respect to LVRT requirements as it behaves differently during voltage sag. For SCIGs to stay connected to the grid, its speed and voltage should be controlled during and post fault events [4][5]. On the other side the DFIG-based wind turbines are very sensitive to voltage dips during grid faults. This is due to the partially-rated back to back power converter. If WPPs are directly connected to grid, it causes the short circuit current surpassing beyond capacities of existing equipment in the grid at some point, resulting into instability from WPPs point of view [6] [7].To satisfy the LVRT requirement of the wind farms, both series and shunt types of devices have been used. Static synchronous compensator (STATCOM) [8], thyristor switched capacitor [9], static VAR compensator [10] have been used as shunt options while Dynamic voltage restorer [11], series dynamic braking resistor (SDBR) [12], unified inter-phase power controller [13], gate controlled series capacitor [14] are the series options. These devices have the capability of improving the transient stability but they are costlier and required huge capital investments. The other options for improving the transient stability and LVRT are fault current limiters (FCLs) as proposed in [15] - [23]. The application of FCLs allows WTs to remain in service, even if fault current exceeds its rated peak value. Moreover, as the magnitude of voltage sag during short circuit event depends upon the magnitude of fault current, an effective FCL connected to the WPP not only limits the large short circuit current but also reduces the voltage sag at Point of Common Coupling (PCC) during fault.

II. GRID CODE REQUIREMENT OF INDIA

The grid code requirement of India is shown in Fig.1 [24]. In this case, as seen from Table I, the voltage at fault V_f should not go below 15% of nominal system voltage. V_{pf} is the voltage after the clearance of fault. T is the minimum time for which the wind farm should remain connected to the grid under the system disturbances. The fault clearing time depends on the voltage level of the system. Table-I shows the voltage level and fault clearing time as per grid code requirement

Revised Manuscript Received on December 30, 2019.
* Correspondence Author
Chintan R. Mehta*, Assistant Professor, Electrical Engineering Department, Institute of Technology, Nirma University, Ahmedabad, India.
Bhavik D. Nathani, Electrical Engineering Department, Institute of Technology, Nirma University, Ahmedabad, India.
Prasad D. Deshpande, Electrical Engineering Department, Institute of Technology, Nirma University, Ahmedabad, India.
Santosh C. Vora, HOD, Electrical Engineering Department, Institute of Technology, Nirma University, Ahmedabad, India.

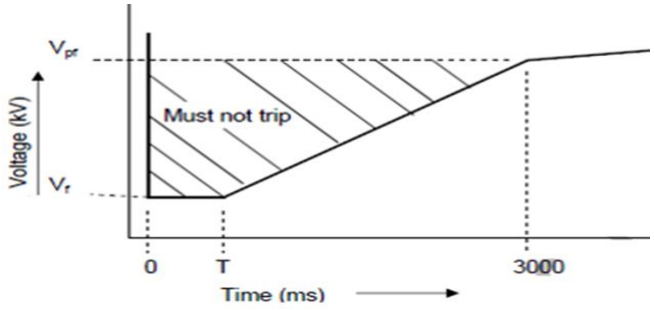

Fig. 1. LVRT requirement as per Indian electricity grid code

Table- I: Fault clearing time and voltage limits

Nominal System Voltage (kV)	Fault Clearing Time T (ms)	V_{pf} (kV)	V_f (kV)
400	100	360	60
220	160	200	33
132	160	120	19.8
110	160	96.25	16.5
66	300	60	9.9

The above LVRT requirements are mandatory for all operators irrespective of type of wind generators used. In this paper, the authors have considered the following two cases.

1. Effects of various FCLs in Transient stability analysis of FSIG based wind farm connected to infinite bus.
2. Effects of various FCLs in Transient stability analysis of a hybrid combination of DFIG & FSIG wind farm connected to infinite bus.

III. WIND TURBINE AND INDUCTION GENERATOR MODELING

The wind turbine generator is divided in to following categories [19][22].

1. Wind turbine model
2. Induction generator model (FSIG, DFIG, PMSG etc)
3. Control system modelling
4. Drive train modelling
5. Pitch angle control

The kinetic energy available from the wind energy is being converted to the mechanical power (P_m).

$$Pm = 0.5\ \rho\ A_w\ C_p\ V^3_W \quad (1)$$

where, ρ is the air density, V_W is the wind speed (*m/s*), Aw= πR^2 is the area covered by the WT blade and *R* is the blade radius in m and C_p is the power coefficient as function of the tip speed ratio(λ) and pitch angle (β). Fig. 2 shows the equivalent circuit of the induction generator [22]. Based on the equivalent circuit, the stator and rotor voltages and currents are expressed as

$$\overrightarrow{v_s} = R_s\overrightarrow{i_s} + \frac{d\overrightarrow{\psi_s}}{dt} + j\omega_s\overrightarrow{\psi_s} \quad (2)$$

$$\overrightarrow{v_r} = R_r\overrightarrow{i_r} + \frac{d\overrightarrow{\psi_r}}{dt} + j(\omega_s - \omega_r)\overrightarrow{\psi_r} \quad (3)$$

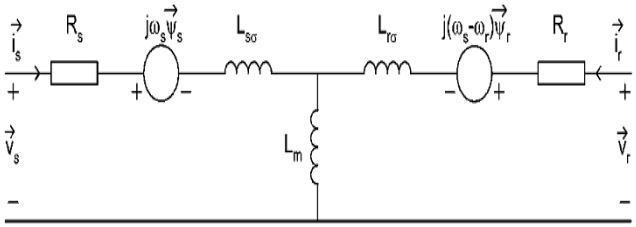

Fig. 2.Equivalent circuit of Induction Generator

$$\overrightarrow{i_s} = \frac{1}{L'_s}[\overrightarrow{\psi_s} - k_s\overrightarrow{\psi_r}] \quad (4)$$

$$\overrightarrow{i_r} = \frac{1}{L'_r}[\overrightarrow{\psi_r} - k_s\overrightarrow{\psi_s}] \quad (5)$$

Where

$$\overrightarrow{\psi_s} = L_s\overrightarrow{i_s} + L_m\overrightarrow{i_r} \text{ and } \overrightarrow{\psi_r} = L_r\overrightarrow{i_r} + L_m\overrightarrow{i_s}$$

$$L'_s = L_{s\sigma} + \frac{L_{r\sigma}L_m}{L_{r\sigma}+L_m}, L'_r = L_{r\sigma} + \frac{L_{s\sigma}L_m}{L_{s\sigma}+L_m}$$

$$k_s = \frac{L_m}{L_s}, k_r = \frac{L_m}{L_r}$$

$$\sigma = 1 - \frac{L_m^2}{L_sL_r} = \text{Leakage factor}$$

$\vec{\psi}_s$ and $\vec{\psi}_r$ term represents flux linkages of stator and rotor respectively. ω_s and ω_r represents stator and rotor angular speed respectively. R_s and R_r represents stator resistance and rotor resistance respectively. L_s is stator inductance, L_r is rotor inductance and they are related to the stator leakage inductance $L_{s\sigma}$ and the rotor leakage inductance $L_{r\sigma}$.

IV. DIFFERENT TYPES OF FAULT CURRENT LIMITERS (FCLs)

The authors have considered the following types of fault current limiters in this paper.

1) Bridge type Fault Current Limiter (BFCL)
2) Non superconducting fault Current Limiter (NSFCL)
3) Capacitive Bridge type Fault Current Limiter (CBFCL)

A. *BFCL Configuration and Operation*

BFCL configuration is proposed by [19]. The BFCL circuit is shown in Fig. 3. BFCL topology consists of diode bridge (D_1 - D_4), a small valued dc reactor L_{dc} with a parallel free-wheeling diode (D_f) and a bypass current limiting reactor L_{sh} in series with a resistor R_{sh}. Under conventional operation, the IGBT switch is closed and the in the one half cycle of electrical frequency the line current flows through A-D_1-L_{dc}-R_{dc}-S_1- D_4-B. During the other half cycle the line current flows through A-D_2-L_{dc}-R_{dc}-S_1-D_3-B. So the current through L_{dc} flows in the same direction and this current is dc current. As the impedance of the parallel path is high, the current through the parallel path is almost zero.

When fault occurs, the controller detects it and turns off the IGBT switch S_1 and the bridge part is isolated from the faulted line, thereby bypassing the fault line current to the parallel path.

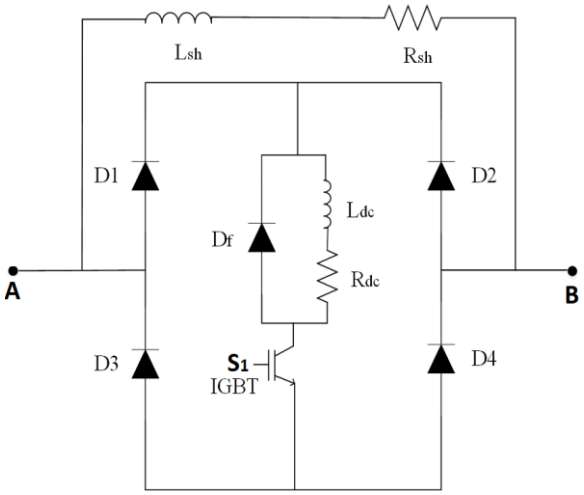

Fig. 3.Circuit of BFCL

The parallel path limits, the fault current and the high impedance of resistance consumes the excess energy from the wind generators to ensure safe operation. Once the fault gets cleared, the controller turns on the IGBT switch S_1 and normal operation of the bridge is restrained.

B. *NSFCL Configuration and Operation*

NSFCL and NBFCL configuration is proposed by [20] [21]. Authors of [21] have proposed NBFCL which does not consider the effects of resistor connected in series with inductor. All other parameters are same as NSFCL. Hence in this paper NSFCL is considered for the analysis purpose. Circuit of NSFCL is shown in Fig. 4.

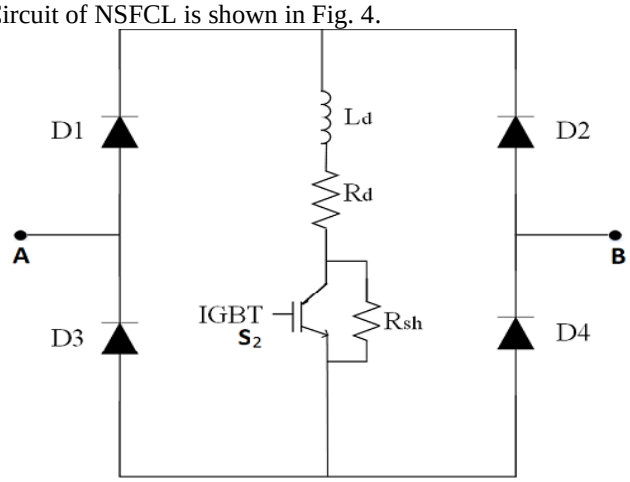

Fig. 4.Circuit of NSFCL

NSFCL topology consists of diode bridge (D_1 - D_4). In this topology, non-superconductor (copper coil) which is designed by a small value of resistor (R_d) and an inductor (L_d) is proposed and is connected in series with a IGBT switch. A resistor (R_{sh}) is connected in shunt with the IGBT switch S_2 for limiting the high current during the fault. Under steady state conditions the IGBT switch S_2 remains closed and the rectifier diode bridge part of the NSFCL carries the line current. When a fault occurs, the line current begins to rise abruptly but is limited by the reactor. At the time of the fault, dc current (i_{dc}) becomes greater than the predefined maximum permissible current (i_{ref}) and the controller of NSFCL opens the IGBT switch S_2. As the IGBT switch is opened, the line current gets bypassed to the shunt path (R_{sh}), thereby limiting the fault current and consuming the excess energy from the DFIG, ensuring system transient stability.

C. *CBFCL Configuration and Operation*

CBFCL configuration is proposed by [22]-[23]. The CBFCL circuit is shown in Fig. 5.

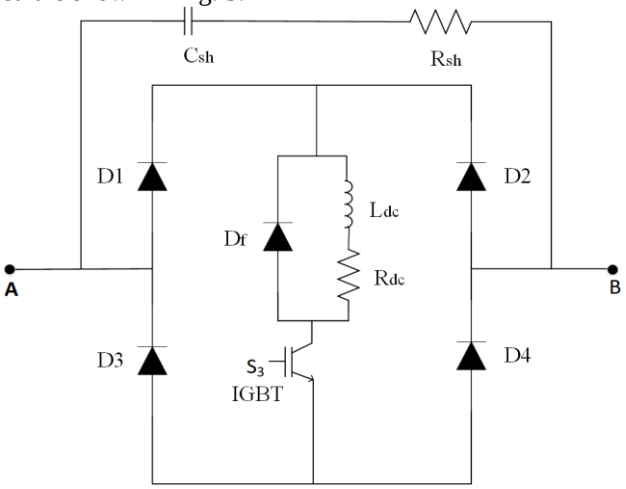

Fig. 5.Circuit of NBFCL

It consists of the limiting impedance which includes a resistor (R_{sh}) in series with capacitor (C_{sh}) connected in shunt with the bridge circuit. The rest of the arrangement is same as the BFCL. The operating principle of CBFCL is the insertion of the capacitive limiting impedance in series with the faulted line during fault conditions. In this paper the authors have considered two different values of DC reactors i.e. ratio of inductance and internal resistance of DC reactors L_{dc}/R_{dc} as τ = 1 s and τ = 5 s to show the impact of different values of DC reactor in the performance of CBFCL.

D. *Control Strategy of Fault Current Limiters (FCLs)*

For designing the control strategy of the various FCLs described in this paper, the parameters taken into consideration are dc current (i_{dc}), reference current (i_{ref}), PCC voltage (V_{pcc}), and the reference voltage (V_{ref}). The control layout of the FCL is rendered in Fig. 6.

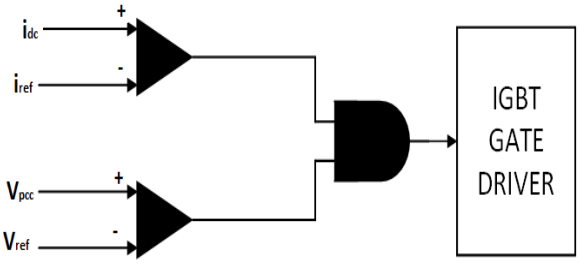

Fig. 6.Control Strategy of IGBT switch

During normal condition, IGBT switch remains closed and the dc current i_{dc} is compared with the reference current (i_{ref}).The value of i_{ref} is set to 1.25 times the value of i_{dc}. At the instance of fault, the dc current i_{dc} becomes greater than the preset reference current (i_{ref}). The control circuit detects this change and opens the IGBT switch. As the IGBT switch opens, the high fault current of the system gets bypassed through the high impedance path and protect the diode bridge. After the clearance of fault, the PCC voltage (V_{pcc}) is compared with the reference voltage (V_{ref}). The reference voltage (V_{ref}) is set to be 0.95 p.u. of the value of the voltage (V_{pcc}). Whenever the PCC voltage (V_{pcc}) is greater than the reference voltage (V_{ref}), the controller sends a signal to the logic controller and then an appropriate gate signal is provided to the IGBT switch again. Hence, the system returns to the normal operating condition. In this paper all the results have been reproduced by the authors for all FCLs and have been compared with the case having no controllers.

V. SYSTEM DESCRIPTION

The SMIB system depicted in Fig. 7 has been considered for simulation study and is simulated in PSCAD/EMTDC.

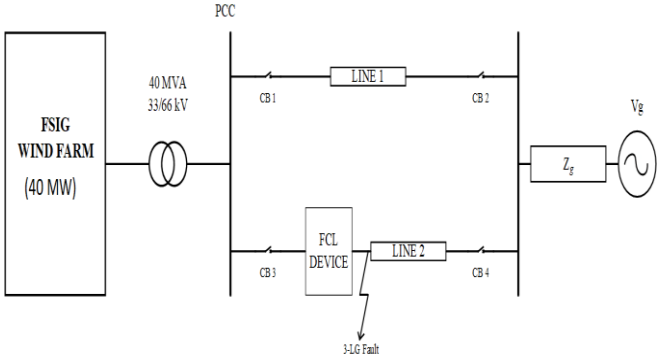

Fig. 7.SMIB test case with FSIG WF

In this case study a FSIG based wind farm generating 40 MW is considered connected to an infinite grid via a double circuit transmission line. The capacity of individual generator is 5 MW. The various FCLs described in Section IV are connected in series with transmission line 2. Various parameters of different FCLs are shown in Table II.

Table- II: Parameters of various FCLs

FCL	L_d (H)	R_d (Ω)	R_{sh} (Ω)	L_{sh} (H)	C_{sh} (μF)
CBFCL (τ = 1)	0.01	0.01	217	-	27
CBFCL (τ = 5)	0.001	0.0002	217	-	27
NSFCL	0.001	0.0002	30	-	-
BFCL	0.001	0.0002	30	0.3	-

To compare the effectiveness of the various FCLs a 3 L-G fault is simulated on Line 2 after the FCLs. The fault is applied at 10 sec and the fault is cleared at 10.15 sec. The breaker operation is also considered for fault isolation and the breakers on line 2 are operated at time t = 10.1s and re-closed at time t = 10.65s after clearing the fault. For the purpose of short circuit analysis the wind speed is considered as constant at 11 m/s to generate the rated power.

The authors have considered following five different cases for analysis.

The cases are as follows:

1) Transient stability analysis without any controller
2) Transient stability analysis with BFCL
3) Transient stability analysis with NSFCL
4) Transient stability analysis with CBFCL (L_{dc}/R_{dc} ratio τ = 1s)
5) Transient stability analysis with CBFCL (L_{dc}/R_{dc} ratio τ =5s)

A. *Transient Stability Analysis for Symmetrical Fault with FSIG Wind Farm*

Fig. 8 shows the RMS voltage, active power output, reactive power output and RMS current respectively at PCC of FSIG based wind farm.

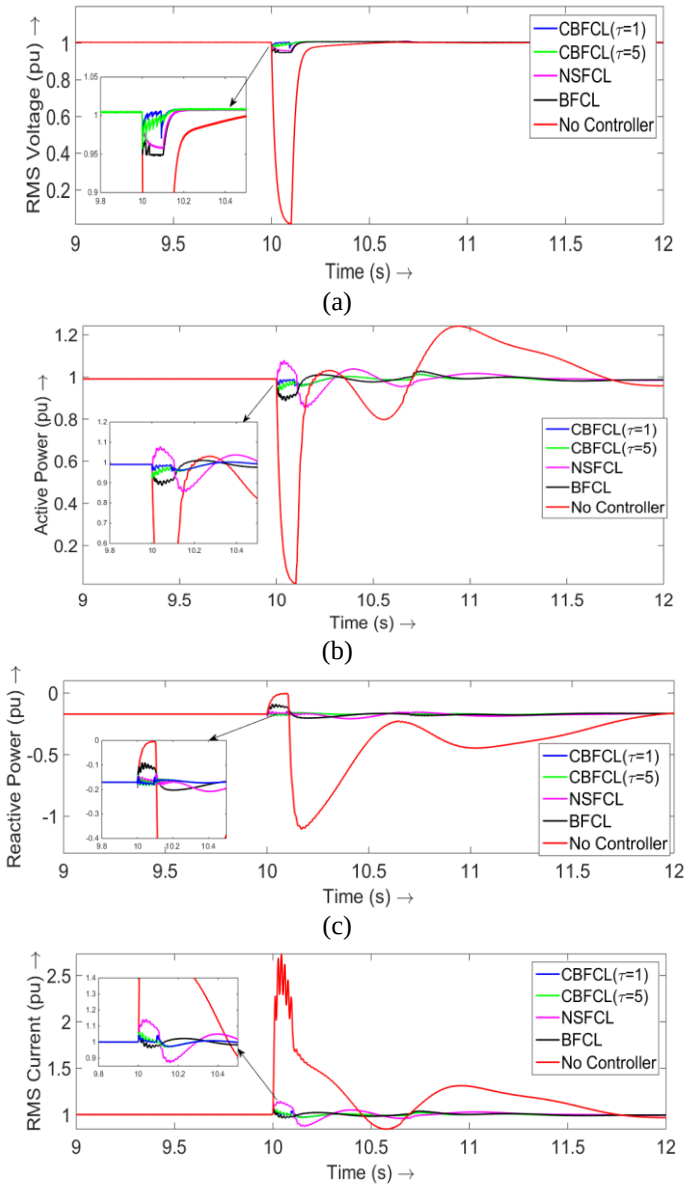

Fig. 8.Simulation response of FSIG wind farm at PCC for 3-LG fault: (a) Terminal Voltage (RMS); (b) Active Power; (c) Reactive Power; (d) RMS Current

Fig. 8a shows the RMS voltage response at PCC. It can be observed that without any fault current limiters, the FSIG terminal voltage reduces approximately to zero and continues at a lower voltage range until the circuit breakers opens. However, when the FCLs are connected to the system, the voltage at PCC improves drastically as seen in Fig. 8a. The RMS voltage in all cases are shown in Table III. All the fault current limiters can maintain the terminal voltage nearly to 0.95 p.u. which is above the requirement of majority of grid codes. But, the simulation results clearly indicates that the performance of the CBFCL with (τ = 1s) is slightly better as compared to other methods.

Fig. 8b shows the active power output of FSIG wind farm. It is observed that without any controller, active power demand to the machine falls down approximately to zero and remains till the opening of breaker. As seen in the Fig. 8b breaker operation gives sudden surge in active power which is affecting the performance of machine. The abrupt rise in active power may force false tripping of associated relays in the system. After considering various FCLs, the variation in active power is drastically improved which can be seen from Table III. The performance of the NSFCL is better compared to other FCLs.

Fig. 8c shows the reactive power exchange between grid and the wind farm. For the case when no FCLs are connected, it can be observed that FSIG absorbs more reactive power from the grid. However, it can be clearly seen that when FCLs are implemented in the system, the variation of reactive power is drastically reduced. The performance of CBFCL with (τ = 1s) is better as compared to all other FCLs.

Fig. 8d shows the simulation results of rms current at the fault. It can be seen that, when no FCLs are connected to the system the peak of the rms current reaches up to 2.731 pu during fault. However, when FCLs are connected to system the peak values of the rms current reduces effectively. Also, it is evident that the performance of CBFCL with (τ = 1s) is better as compared to other FCLs.

Fig. 9 shows the RMS voltage, Active power, Reactive Power and RMS current in line 1. Line 1 is healthy line and the response of line 1 also improves with the implementation of FCLs. The reactive power is absorbed by line 1 for all FCLs except CBFCL which supplies the reactive power to the system. The FCLs will be ineffective in case of only one transmission line (i.e. no parallel transmission line) as the fault current is fed from line 1. As seen from the response under no FCLs the rms current through line 1 rises drastically as the entire fault current is fed from the grid through line 1.

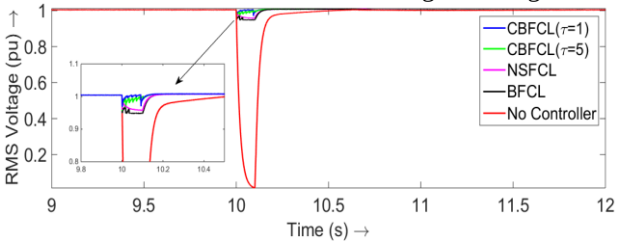

(a)

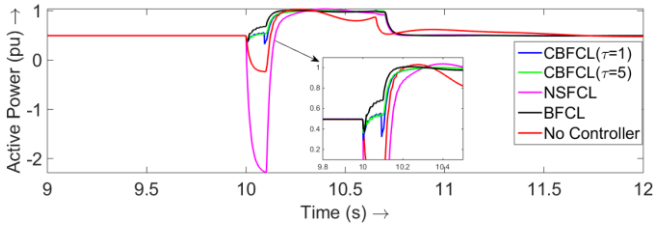

(b)

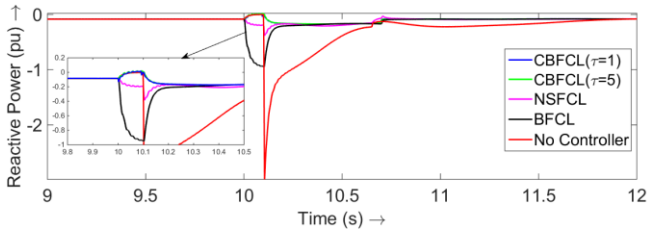

(c)

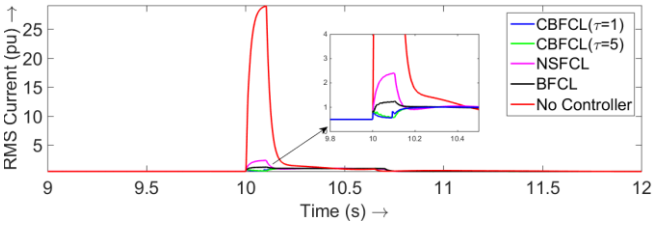

(d)

Fig. 9 Simulation response on line 1 of FSIG wind farm: (a) Terminal Voltage; (b) Output Active Power; (c) Output Reactive Power; (d) RMS Current

B. *Transient Stability Analysis of a Wind Farm Consisting Hybrid Combination of DFIG & FSIG for Symmetrical Fault*

In the literature available, the effects of FCLs are shown in either FSIG or DFIG based wind farms for symmetrical and asymmetrical faults. In this section the effects of FCLs connected to a wind farm consisting of a hybrid combination of FSIG and DFIG connected to infinite bus for symmetrical fault as all wind farms nowadays consists various combinations of wind turbine generators.

The aggregated power output of the wind farm is considered as 40 MW at PCC assuming both types of WTGs generates 20 MW each. The system considered for this case is shown in the Fig. 10. The system parameters are shown in Table - V in Appendix. A 3 L-G fault is simulated at line 2 and the performance of all FCLs during fault is analyzed. All other conditions remains same as case A.

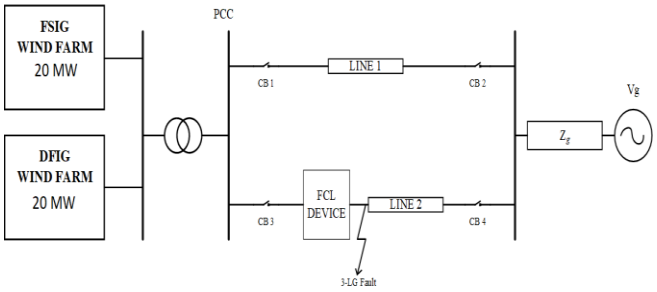

Fig. 10 SMIB test case for an aggregated hybrid wind farm of DFIG & FSIG

Fig. 11 shows the responses of RMS voltage, active power, reactive power and RMS current at PCC.

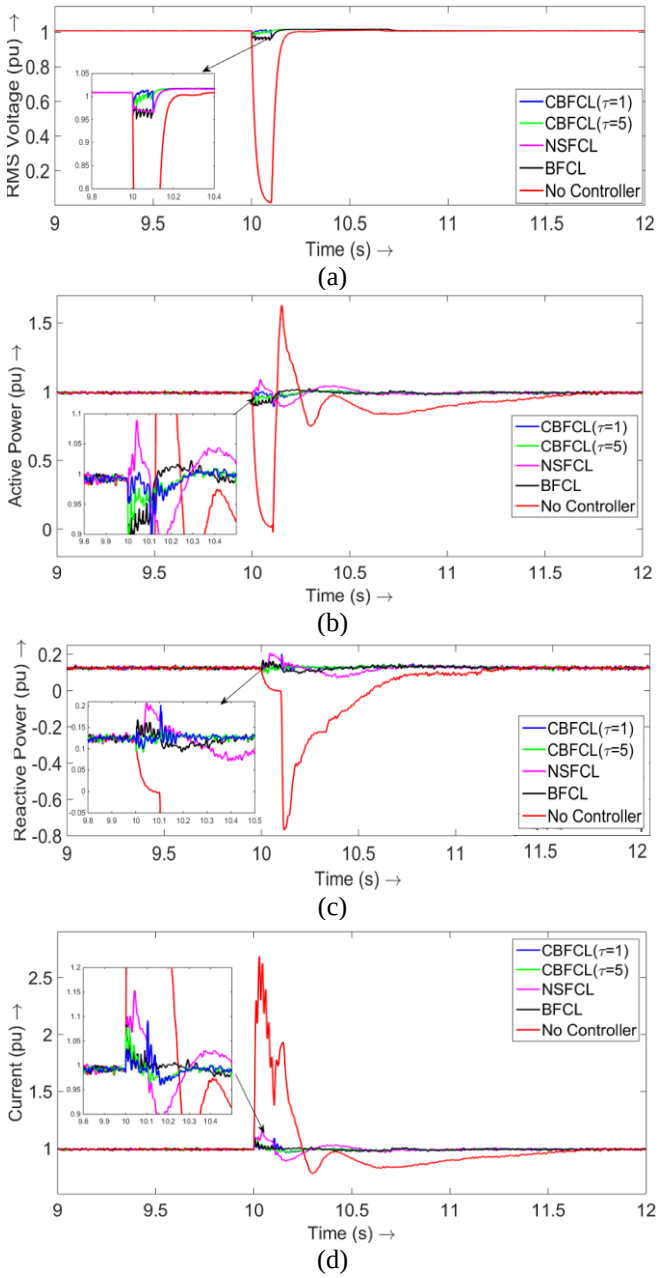

Fig. 11 Simulation response of wind farm at PCC for 3 L-G fault considering hybrid wind farm of FSIG and DFIG: (a) Terminal Voltage (RMS); (b) Active Power; (c) Reactive Power; (d) RMS Current

Fig. 11a shows that the terminal voltage reaches to almost zero at the instant of 3 L-G fault when no FCLs are considered. However, when FCLs are taken in to consideration the voltage profile improves. Although it can be observed from the results that all the FCLs improves the voltage. CBFCL with a τ of 1s is showing the best performance as compared to other FCLs.

Fig. 11b shows the total active power output of the WFs. The active power output by the WF reaches to zero during fault. All the FCLs prevents the rapid active power dip. The active power at PCC is reduced from 0.9556 p.u. to 0.8891 pu for CBFCL with a τ of 1s as compared to case A.

The performance of NSFCL is better and has the minimum power dip during fault. Fig. 11c shows the reactive power exchanged between the WF and the grid. As seen, the absorbed reactive power from the grid without any series device is -0.769 pu, it is effectively reduced when series devices are accounted. As seen in Table IV, wind farm consisting of hybrid combination of FSIG and DFIG supplies the reactive power to grid unlike the case 1 which absorbs the reactive power from grid. It is evident from the Fig. 11c that NSFCL provides the reactive power support to the grid as compared to other FCLs.

The rms current is shown in Fig. 11d. From the figure it is evident that the performance of CBFCL (τ = 5s) is superior as compared to other FCLs.

Fig. 12 represents the RMS voltage, Active power, Reactive Power and RMS current in line 1. Line 1 is healthy line and the response of line 1 also improves with the implementation of FCLs.

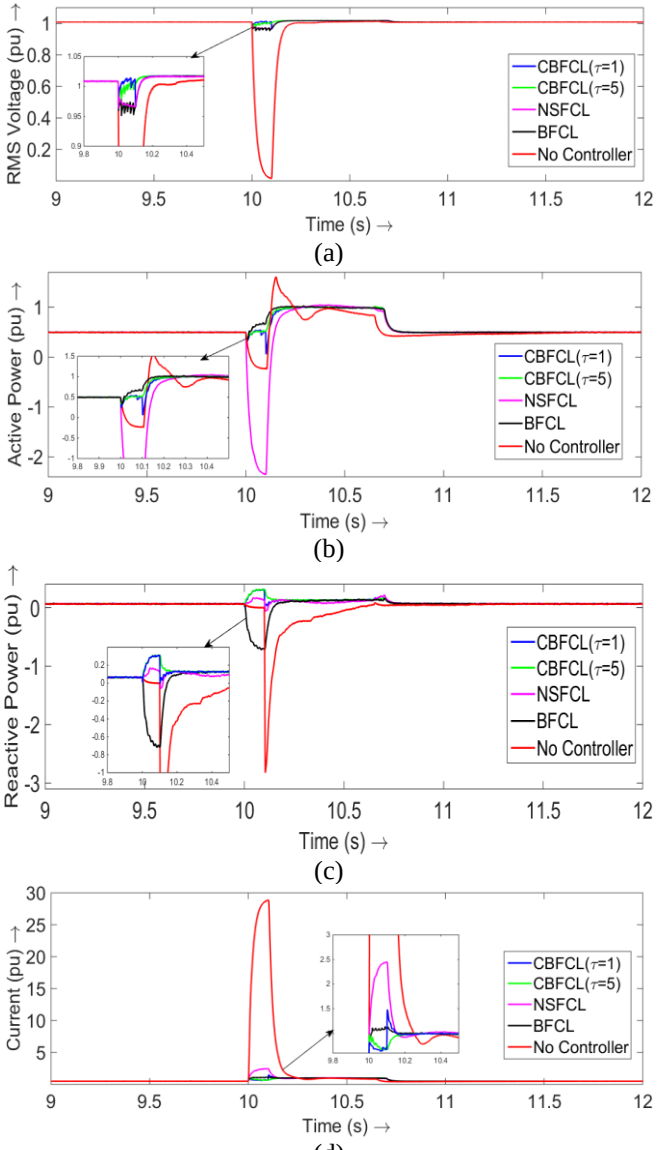

Fig. 12 Simulation response at line 1 for 3-LG fault considering hybrid wind farm of FSIG and DFIG: (a) Terminal Voltage (RMS); (b) Active Power; (c) Reactive Power; (d) RMS Current

C. *Comparison of Case-1 and Case-2*

In this paper, the authors have considered two cases. The impact of different types of generators is clearly visible in case of reactive power. The FSIG based wind farm consumes reactive power with all FCLs but when DFIG and FSIG are considered in combination the reactive power profile is improved as DFIG consists of capacitor in DC link of RSC and GSC. The active power variation at the fault is also visible in case of CBFCL. All the results at PCC are shown in Table III and IV.

Table- III: RESULTS for FSIG based WF with FCLs

FCL	V_{PCC} (p.u.)	P (p.u.)	Q (p.u.)	I_{PCC} (p.u.)
CBFCL (τ = 1)	0.9686	0.9556	-0.144	1.045
CBFCL (τ = 5)	0.9568	0.9196	-0.139	1.064
NSFCL	0.9571	1.078	-0.136	1.142
BFCL	0.947	0.8854	-0.0898	1.067
No Controller	0.0146	0.0163	-0.0026	2.731

Table- IV: RESULTS for aggregated hybrid wind farm of FSIG and DFIG based WF with FCLs

FCL	V_{PCC} (p.u.)	P (p.u.)	Q (p.u.)	I_{PCC} (p.u.)
CBFCL (τ = 1)	0.9657	0.8891	0.202	1.092
CBFCL (τ = 5)	0.9625	0.888	0.140	1.079
NSFCL	0.9626	1.09	0.207	1.153
BFCL	0.9506	0.8957	0.168	1.083
No Controller	0.0135	-0.0255	-0.769	2.685

VI. CONCLUSION

The work presented in this research paper indicates the effectiveness of the series connected FCLs for FSIG and a combination of FSIG and DFIG in wind farm considering symmetrical fault. From the simulation results presented in this research work it can be deduced that the FCLs and in in particular CBFCL with a time constant of 1s proves to be effective compared to other FCLs. In conclusion the following point can be deduced after all simulation results:

1. The BFCL and NSFCL proves to be the promising FCLs in the FSIG based WF, as these devices are capable of reducing the fault current and maintains the voltage level well above the requirement of grid codes for a 3 L-G fault.
2. The CBFCL is the other favorable solution for enhancing the LVRT performance of FSIG based WFs. The consideration of CBFCL with time constant of 1s & 5s is shown in this paper. In both the cases the CBFCL has minimized the fault current, and also minimized the oscillations of active power of the FSIG WF and has maintained the voltage profile above 0.95p.u.for 3 L-G fault.
3. The paper shows responses of the wind farm consisting of the hybrid combination of DFIG and FSIG at PCC. FSIG have squirrel cage induction generator while DFIG has wound rotor induction generator. The difference is clearly visible in case of reactive power support provided to the grid in the combination of FSIG and DFIG in the wind farm.
4. The responses of the line 1 (healthy line) is also shown in both the cases. It can be also concluded that all FCLs will be effective only if parallel transmission lines are considered in the system.

REFERENCES

1. Peter E.Sutherland, “Ensuring stable operation with grid codes: A look at Canadian wind Farm Interconnections,” IEEE Industry Applications Magazine, 2016.
2. M. Tsili, S. Papathanassiou, “A review of grid code technical requirements for wind farms,” IET Renewable Power Generation, Vol. 3, Issue 3, 2009.
3. Marco Liserre, Roberto Cardenas, Marta Molinas, Jose Rodriguez, “Overview of Multi-MW Wind Turbines and Wind Parks,” IEEE Transactions on Industrial Electronics, Vol. 58, No. 4, April 2011.
4. M.S. El-Moursi, “Fault ride through capability enhancement for self-excited induction generator-based wind parks by installing fault current limiters,” IET Renewable Power Generation, 2011.
5. J. Pedra, F. Corcoles, Ll. Monjo, S. Bogarra and A. Rolan, “On Fixed-Speed WT Generator Modeling for Rotor Speed Stability Studies,” IEEE Transactions on Power Systems, Vol. 27, No. 1, February 2012.
6. Eduard Muljadi, Nader Samaan, Vahan Gevorgian, Jun Li, Subbaiah Pasupulati, “Short Circuit Current Contribution for Different Wind Turbine Generator Types,” IEEE Power and Energy Society General Meeting, 2010.
7. F. D. Kanellos and John Kabouris, “Wind Farms Modeling for Short-Circuit Level Calculations in Large Power Systems,” IEEE Transactions on Power Delivery, Vol. 24, No. 3, July 2009.
8. M.M.A Mahfouz, Mohamed A.H. El-Sayed,, “Static synchronous compensator sizing for enhancement of fault ride-through capability and voltage stabilization of fixed speed wind farms,” IET Renewable Power Generation, Vol. 8, Issue. 1, 2014.
9. Jiajia Ren, Yinghong Hu, Yanchao Ji, Chuang Liu, “Low Voltage Ride-through Control for Fixed Speed Wind Generators under Grid Unbalanced Fault,” Twenty-Seventh Annual IEEE Applied Power Electronics Conference and Exposition (APEC), 2012.
10. Marta Molinas, Joon Are Suul and Tore Undeland, “Low Voltage Ride Through of Wind Farms With Cage Generators: STATCOM Versus SVC,” IEEE Transaction on Power Electronics, Vol. 23, No. 3, May 2008.
11. Andres E. Leon, Marcelo F. Farias, Pedro E. Battaiotto, Jorge A. Solsona and Maria Ines Valla, “Control Strategy of a DVR to Improve Stability in Wind Farms Using Squirrel-Cage Induction Generators,” IEEE Transactions on Power Systems, Vol. 26, No. 3, August 2011.
12. Andrew Causebrook, David J. Atkinson and Alan G. Jack, “Fault Ride-Through of Large Wind Farms Using Series Dynamic Braking Resistors,” IEEE Transactions on Power Systems, Vol. 22, No. 3, August 2007.
13. Mehdi Firouzi, Gevork B. Gharehpetian, Seid Babak Mozafari, “Application of UIFC to improve power system stability and LVRT capability of SCIG-based wind farms,” IET Generation, Transmission and Distribution, Vol. 11, Issue. 9, 2017.
14. Hossein Ali Mohammadpour, Amin Ghaderi, Hassan Mohammadpour, Mohd. Hasan Ali, “Low voltage ride-through enhancement of fixed-speed wind farms using series FACTS controllers,” Sustainable Energy Technologies and Assessments, 2015.
15. Lin Ye and Liang Zhen Lin, “Study of Superconducting Fault Current Limiters for System Integration of Wind Farms,” IEEE Transactions on Applied Superconductity, Vol. 20, No. 3, June 2010.
16. M. Firouzi and G. B. Gharehpetian, “Improving Fault Ride-Through Capability of Fixed-Speed Wind Turbine by Using Bridge-Type Fault Current Limiter,” IEEE Transactions on Energy Conversion, Vol. 28, No. 2, June 2013.

17. Gilmanur Rashid, Mohd. Hasan Ali, "Nonlinear Control-Based Modified BFCL for LVRT Capacity Enhancement of DFIG-Based Wind Farm," IEEE Transactions on Energy Conversion, Vol. 32, No. 1, March 2017.
18. M. E. Hossain, "Improvement of transient stability of DFIG based wind generator by using of resistive solid state fault current limiter," Ain Shams Engineering Journal, 2017.
19. Gilamanur Rashid and Mohd. Hasan Ali, "Transient Stability Enhancement of Doubly Fed Induction Machine-Based Wind Generator by Bridge-Type Fault Current Limiter," IEEE Transactions on Energy Conversion, Vol. 30, No. 3, September 2015.
20. M. E. Hossain, "Performance analysis of diode-bridge-type non-superconducting fault current limiter in improving transient stability of DFIG based variable speed wind generator," Electric Power Systems Research, 2017.
21. M. E. Hossain, "A non-linear controller based new bridge type fault current limiter for transient stability enhancement of DFIG based Wind Farm," Electric Power Systems Research, 2017.
22. M. Firouzi and G. B. Gharehpetian, "LVRT Performance Enhancement of DFIG-Based Wind Farms by Capacitive Bridge-Type Fault Current Limiter (CBFCL)," IEEE Transactions on Sustainable Energy, 2017.
23. M. Firouzi, "A modified capacitive bridge-type fault current limiter (CBFCL) for LVRT performance enhancement of wind power plants," International Transactions on Electrical Energy Systems, 2017.
24. https//www.niwe.res.in

AUTHORS PROFILE

Chintan R. Mehta is currently working as Assistant Professor in Electrical Engineering Department at Institute of Technology, Nirma University, Ahmedabad. He has obtained B. E. and M.E. in Electrical Engineering from Gujarat University. He has many research publication in various national and international journals and conferences to his credit. His main research interests includes grid integration of large scale renewable energy systems, power system stability analysis, distributed generation, power system planning, operation, and control.

Bhavik D. Nathani was born in Anjar, Gujarat, India in June 1995. He received the B.E. degree in Electrical Engineering from Kadi Sarva Vishwavidyalaya, Gandhinagar, Gujarat, India, in 2016, and the M.Tech degree with distinction in Electrical Engineering (specialization in Electrical Power Systems) from Institute of Technology, Nirma University, Ahmedabad, Gujarat, India in 2019. His main research interests includes grid integration of large scale renewable energy systems, power system stability analysis, power system protection.

Prasad D. Deshpande was born in Dahod, Gujarat, India in October 1995. He received the B.E. degree in Electrical Engineering from Gujarat Technological University, Ahmedabad, Gujarat, India, in 2017, and the M.Tech degree with distinction in Electrical Engineering (specialization in Electrical Power Systems) from Institute of Technology, Nirma University, Ahmedabad, Gujarat, India in 2019. His main research interests includes grid integration of large scale renewable energy systems, power system stability analysis, distributed generation, power system design, planning, operation, and control.

Santosh C. Vora is working as Head of Electrical Engineering Department at Institute of Technology, Nirma University, Ahmedabad. He has obtained Ph.D. from Indian Institute of Science, Bangalaore. He has many research publications to his credit in international and national journals & conferences. His main research interests includes electeical machines, High voltage engineering, Renewable energy integration in power grid and Power systems transients. He is reviewer in many international journals.

APPENDIX

Table-V: System parameters

Generator Type	FSIG	DFIG
Rated power (MVA)	5	5
Rated voltage (kV)	0.69	0.69
Inertia Constant (s)	4.32	3
Stator resistance (pu)	0.0054	0.0074
Wound rotor resistance (pu)	0.00607	0.0061
Magnetizing inductance (pu)	4.5	4.3621
Stator leakage inductance (pu)	0.1	0.1022
Wound rotor leakage inductance (pu)	0.11	0.1123